# Clearance of Alzheimer's amyloid-$\beta_{1\text{-}40}$ peptide from brain by LDL receptor–related protein-1 at the blood-brain barrier

Masayoshi Shibata,[1] Shinya Yamada,[1] S. Ram Kumar,[1] Miguel Calero,[2] James Bading,[3] Blas Frangione,[2] David M. Holtzman,[4] Carol A. Miller,[5] Dudley K. Strickland,[6] Jorge Ghiso,[2] and Berislav V. Zlokovic[1,7]

[1]Department of Neurological Surgery, Keck School of Medicine of the University of Southern California, Los Angeles, California, USA
[2]Department of Pathology, New York University Medical Center, New York, New York, USA
[3]Department of Radiology, Keck School of Medicine of the University of Southern California, Los Angeles, California, USA
[4]Department of Neurology, Washington University School of Medicine, St. Louis, Missouri, USA
[5]Department of Pathology, Keck School of Medicine of the University of Southern California, Los Angeles, California, USA
[6]Department of Vascular Biology, Holland Laboratories, American Red Cross, Rockville, Maryland, USA
[7]Division of Neurovascular Biology, Center for Aging and Developmental Biology of the University of Rochester Medical School, Rochester, New York, USA

Address correspondence to: Berislav V. Zlokovic, Division of Neurovascular Biology, Aab Institute of Biomedical Sciences, Center for Aging and Developmental Biology, University of Rochester Medical School, 601 Elmwood Avenue, Box 645, Rochester, New York 14642, USA. Phone: (716) 273-3132; Fax: (716) 273-3133; E-mail: Berislav_Zlokovic@urmc.rochester.edu.

Elimination of amyloid-β peptide (Aβ) from the brain is poorly understood. After intracerebral microinjections in young mice, $^{125}$I-Aβ$_{1\text{-}40}$ was rapidly removed from the brain ($t_{1/2} \leq 25$ minutes), mainly by vascular transport across the blood-brain barrier (BBB). The efflux transport system for Aβ$_{1\text{-}40}$ at the BBB was half saturated at 15.3 nM, and the maximal transport capacity was reached between 70 nM and 100 nM. Aβ$_{1\text{-}40}$ clearance was substantially inhibited by the receptor-associated protein, and by antibodies against LDL receptor–related protein-1 (LRP-1) and α$_2$-macroglobulin (α$_2$M). As compared to adult wild-type mice, clearance was significantly reduced in young and old apolipoprotein E (apoE) knockout mice, and in old wild-type mice. There was no evidence that Aβ was metabolized in brain interstitial fluid and degraded to smaller peptide fragments and amino acids before its transport across the BBB into the circulation. LRP-1, although abundant in brain microvessels in young mice, was downregulated in older animals, and this downregulation correlated with regional Aβ accumulation in brains of Alzheimer's disease (AD) patients. We conclude that the BBB removes Aβ from the brain largely via age-dependent, LRP-1–mediated transport that is influenced by α$_2$M and/or apoE, and may be impaired in AD.

*J. Clin. Invest.* **106**:1489–1499 (2000).

## Introduction

Deposition of amyloid-β peptide (Aβ) in the brain occurs during normal aging and is accelerated in patients with Alzheimer's disease (AD). Aβ is central to the pathology of AD, and is the main constituent of brain parenchymal and vascular amyloid (1–6). Aβ extracted from senile plaques contains mainly Aβ$_{1\text{-}40}$ and Aβ$_{1\text{-}42}$ (7), whereas vascular amyloid is predominantly Aβ$_{1\text{-}39}$ and Aβ$_{1\text{-}40}$ (8). Several sequences of Aβ were found in both lesions (9–11). A major soluble form of Aβ, which is present in the blood, cerebrospinal fluid (CSF) (12–14), and brain (15–16) is Aβ$_{1\text{-}40}$. In the circulation, CSF, and brain interstitial fluid (ISF), soluble Aβ may exist as a free peptide or be associated with different transport binding proteins such as apolipoproteins J (apoJ) (17–18) and E (apoE) (19), transthyretin (20), lipoproteins (21), albumin (22), and α$_2$-macroglobulin (α$_2$M) (23).

The neuronal theory argues that soluble brain-derived Aβ is a precursor of Aβ deposits. Neuronal cells secrete Aβ in culture (24), which supports this view. An increase in soluble Aβ in AD and Down syndrome brains precedes amyloid plaque formation (15, 25, 26) and correlates with the development of vascular pathology (27). Several cytosolic proteases that may degrade intracellular Aβ in vitro cannot degrade extracellular Aβ from brain ISF (28) or CSF (29) in vivo. An exception to this is enkephalinase, which may degrade Aβ$_{1\text{-}42}$ from brain ISF (28). However, the physiological importance of this degradation in vivo remains unclear, because the peptide was studied at extremely high pharmacological concentrations (30).

It has been suggested that decreased clearance of Aβ from brain and CSF is the main cause of Aβ accumulation in sporadic AD (31). Because Aβ is continuously produced in the brain, we hypothesized that an effi-

cient clearance mechanism or mechanisms must exist at the blood-brain barrier (BBB) to prevent its accumulation and subsequent aggregation in the brain. Cell-surface receptors such as the receptor for advanced glycation end products (RAGE) (32–33), scavenger receptor type A (SR-A) (34), LDL receptor–related protein-1 (LRP-1) (35–38), and LRP-2 (39) bind Aβ at low (nanomolar) concentrations as free peptide (RAGE, SR-A) and/or in complex with $\alpha_2 M$, apoE, or apoJ (LRP-1, LRP-2). RAGE and SR-A regulate brain endothelial endocytosis and transcytosis of Aβ that is initiated at the luminal side of the BBB (33), whereas LRP-2 mediates BBB transport of plasma Aβ complexed to apoJ (39). The role of vascular receptors and BBB transport in the removal of brain-derived Aβ is unknown.

In this study, we developed a brain tissue clearance technique in mice based on a model used previously in the rabbit (40). This technique was used to determine in vivo the efflux rates of $A\beta_{1-40}$ from the CNS as a function of time and concentration of peptide, and to characterize vascular transport and/or any receptor-mediated efflux mechanisms involved in elimination of brain-derived Aβ across the BBB. The study focused on LRP-1 and its ligands, $\alpha_2 M$ and apoE, first because they promote Aβ clearance in smooth muscle cells (35), neurons (36, 38), and fibroblasts (37); and second, because apoE4 is a definite risk factor, and $\alpha_2 M$ is a possible risk factor for AD (41–42).

## Methods

*Synthetic peptide and radioiodination*. Peptide DAEFRHDS-GYEVHHQKLVFFAEDVGSNKGAIIGLMVGGVV ($A\beta_{1-40}$) homologous to residues 672–711 of Aβ-precursor protein 770 was synthesized at the W.M. Keck Facility at Yale University using *N-t*-butyloxycarbonyl chemistry. The peptide was purified by HPLC. Aliquots of the final products were lyophilized and stored at –20°C until use. Radioiodination was carried out with $Na^{125}I$ and IodoBeads (Pierce Chemical Co., Rockford, Illinois, USA), and the resulting components were resolved by HPLC (39). Aliquots of radiolabeled $A\beta_{1-40}$ were kept at –20°C for a maximum of 4 weeks before use. The HPLC analysis confirmed that more than 99% of radioactivity was present in the form of nonoxidized monomeric peptide.

*Brain clearance model in mice*. Experiments were performed on male C57BL/6 wild-type mice, 8–10 weeks old and 9–10 months old, and on male apoE knockout (apoE KO) mice on a C57BL/6 background (Taconic Farms, Germantown, New York, USA) that were also 8–10 weeks old and 9–10 months old. CNS clearance of radiolabeled $A\beta_{1-40}$ and the inert polar marker inulin was determined as described below (40, 43).

A stainless steel guide cannula was implanted stereotaxically into the right caudate nucleus of mice anesthetized with 60 mg/kg intraperitoneal sodium pentobarbital). Coordinates for the tip of the cannula were 0.9 mm anterior and 1.9 mm lateral to bregma, and 2.9 mm below the surface of the brain. The guide cannula and screw were fixed to the skull with methylmethacrylate

(Plastics One Inc., Roanoke, Virginia, USA), and a stylet was introduced into the guide cannula. Animals were observed for 1 week before radiotracer studies.

For radioisotope injection, animals were reanesthetized, and an injector cannula (Plastics One Inc.) was attached to a 10-μl gas-tight microsyringe (Hamilton Co., Reno, Nevada, USA) using 24-gauge Teflon tubing (Small Parts Inc., Miami Lake, Florida, USA). The amount of injected tracer was determined accurately using a micrometer to measure linear displacement of the syringe plunger in the precalibrated microsyringe. Tracer fluid (0.5 μl) containing $^{125}I$-$A\beta_{1-40}$ at concentrations varying from 0.05 nM to 120 nM was injected over a period of 5 minutes, along with [$^{14}C$]inulin. When the effect of different molecular reagents was tested, those were injected simultaneously with the radiolabeled peptides.

Time response was studied with $^{125}I$-$A\beta_{1-40}$ from 10 minutes to 300 minutes; dose-dependent effects were determined at 30 minutes. The effects of different molecular reagents that may potentially inhibit $^{125}I$-$A\beta_{1-40}$ clearance were studied at 30 minutes. Among the reagents studied was the rabbit anti–human LRP-1 Ab designated R777, which was affinity purified on a Sepharose–LRP-1 heavy-chain column as described (44). R777 immunoprecipitates mouse LRP-1, as we described (44), and blocks LRP-1–mediated uptake of amyloid β precursor protein (APP) and thrombospondin in murine fibroblasts (45, 46). Another studied reagent that may inhibit $^{125}I$-$A\beta_{1-40}$ clearance is receptor-associated protein (RAP; kindly provided by G. Bu, Washington University). We also studied the rabbit anti–mouse $\alpha_2 M$ Ab designated YNRMA2M, which is specific for mouse $\alpha_2 M$ as demonstrated by radial immunodiffusion and immunoelectrophoresis (Accurate Chemical & Scientific Corp., Westbury, New York, USA); a rabbit anti–rat gp330 affinity-purified IgG designated Rb6286, which crossreacts with mouse LRP-2 as reported (47) (kindly provided by Scott Argraves, University of South Carolina Medical School, Charleston, South Carolina, USA); a rabbit anti-human RAGE Ab that crossreacts with mouse RAGE (32) (kindly provided by D. Stern, Columbia University, New York, New York, USA), and fucoidin (Sigma Chemical Co., St. Louis, Missouri, USA).

*Tissue sampling and radioactivity analysis*. Brain, blood, and CSF were sampled and prepared for radioactivity analysis. Degradation of $^{125}I$-$A\beta_{1-40}$ was initially studied by trichloroacetic acid (TCA) precipitation assay. Previous studies with $^{125}I$-$A\beta_{1-40}$ demonstrated an excellent correlation between TCA and HPLC methods (33, 48–51). Brain, plasma, and CSF samples were mixed with TCA (final concentration 10%) and centrifuged at 24,840 *g* at 4°C for 8–10 minutes. Radioactivity in the precipitate, water, and chloroform fractions was determined in a gamma counter (Wallac Finland Oy, Turku, Finland). The $^{125}I$-$A\beta_{1-40}$ injected into the brain was more than 97% intact, according to TCA analysis.

Degradation of $^{125}I$-$A\beta_{1-40}$ in the brain was further

studied by HPLC and SDS-PAGE analysis. After intracerebral injections of $^{125}$I-A$\beta_{1-40}$, brain tissue was homogenized in PBS containing protease inhibitors (0.5 mM phenylmethylsulfonyl fluoride, 1 µg/ml leupeptin, and 1 mM $p$-aminobenzamidine), and then centrifuged at 100,000 $g$ for 1 hour at 4°C. The supernatant was then lyophilized. The resulting material was dissolved in 0.005% trifluoroacetic acid (TFA) in water at pH 2 before injection onto a Vydac C4 column (The Separations Group, Hesperia, California, USA). The separation was achieved with a 30-minute linear gradient of 25–83% acetonitrile in 0.1% TFA at a flow rate of 1 ml/min, as we have described (51). Under these conditions, the A$\beta_{1-40}$ standard eluted at 14.5 minutes. Column eluants were monitored at 214 nm. The eluted fractions were collected and counted. The $^{125}$I-A$\beta_{1-40}$ injected into the brain was greater than 97% intact according to HPLC analysis, confirming the results of TCA analysis.

For SDS-PAGE analysis, TCA-precipitated samples were resuspended in 1% SDS, vortexed, and incubated at 55°C for 5 minutes. Samples were then neutralized, boiled for 3 minutes, homogenized, and analyzed by electrophoresis in 10% Tris-tricine gels, followed by fluorography. Lyophilized HPLC fractions were resuspended in sample buffer, neutralized, boiled, and electrophoresed as we have reported (39).

*Calculations of clearance rates.* The analysis of curves of radioactivity disappearance from the brain was as reported (40, 43). The percentage of radioactivity remaining in the brain after microinjection was determined as

**(Equation 1)** $\quad$ % Recovery in brain = $100 \times (N_b/N_i)$

where $N_b$ is the radioactivity remaining in the brain at the end of the experiment, and $N_i$ is the radioactivity injected into the brain.

In all calculations, the dpm values for [$^{14}$C]inulin and the cpm values for TCA-precipitable $^{125}$I radioactivity were used. Inulin was studied as a metabolically inert polar reference marker that is neither transported across the BBB nor retained by the brain (40); its clearance rate, $k_{inulin}$, provides a measure of the ISF bulk flow and is calculated as

**(Equation 2)** $\quad$ $N_{b(inulin)}/N_{i(inulin)} = \exp^{(-k_{inulin} \times t)}$

In the case of A$\beta$, there are two possible physiological pathways of elimination: direct transport across the BBB into the bloodstream, and elimination via ISF bulk flow into the CSF and cervical lymphatics. It is also possible that A$\beta$ is retained within the brain by binding to its cell-surface receptors directly as a free peptide, and/or by binding to different transport proteins. Thus, according to the model, the fraction of A$\beta$ remaining in the brain can be expressed as

**(Equation 3)** $\quad$ $N_{b(A\beta)}/N_{i(A\beta)} = (a_1 + a_2) \times e^{-k1 \times t}$

where $a_1 = k_2/(k_1 + k_2)$ and $a_2 = k_1/(k_1 + k_2)$, and $k_1$ and $k_2$ denote the fractional coefficients of total efflux from the brain and retention within the brain, respectively.

The fractional rate constant of A$\beta$ efflux across the BBB from brain parenchyma can be calculated by knowing the fractional rate coefficient of total efflux of A$\beta$ and inulin as

**(Equation 4)** $\quad$ $k_3 = k_1 - k_{(inulin)}$

i.e., as the difference between the fractional rate constant for total efflux of A$\beta$ and the fractional rate constant of inulin. The half-saturation concentration for the elimination of A$\beta$ via transport across the BBB, $k_{1/2}$, was calculated from the equation

**(Equation 5)** $\quad$ $[1 - (N_b/N_i)] \times 100 = Cl_{max}/(k_{1/2} + N_i)$

where $Cl_{max}$ represents the maximal efflux capacity for the saturable component of A$\beta$ clearance across the BBB, corrected for peptide clearance by the ISF flow. $Cl_{max}$ is expressed as a percentage of the injected dose, $[1 - (N_b / N_i)] \times 100$, cleared from brain by saturable BBB transport over 30 minutes.

The MLAB mathematical modeling system (Civilized Software Inc., Silver Spring, Maryland, USA) was used to fit the compartmental model to the disappearance curves or percent recovery data with inverse square weight.

*Immunocytochemical analysis in mice.* Expression of LRP-1 and $\alpha_2$M in mouse brain was studied by immunohistochemical analysis. Fresh-frozen, acetone-fixed brain sections of 2-month-old and 9-month-old wild-type and apoE KO mice were stained using anti-human LRP R777 Ab that crossreacts with mouse LRP-1 (44–46) (1.5 mg/ml; 1:300 dilution), and anti-mouse $\alpha_2$M Ab (as described above, 1:250 dilution). R777 was affinity purified over a Sepharose–LRP-1 heavy-chain column, as described (44). The number of positive vessels was counted in ten random fields by two independent blinded observers, and was expressed as percentage per square millimeter of section. The extent and intensity of staining in cellular elements was quantitated using the ESECO Digimatic Universal Imaging System (Electronic Systems Engineering Co., West Chester, Pennsylvania, USA) and NIH imaging systems. Microvessels were carefully excluded from the quantitation by suitably varying the magnitudes of measurement. The relative intensity of cellular staining (excluding the microvasculature) in brain sections of young mice was arbitrarily normalized to 1 for purposes of comparison. Routine controls included sections prepared without primary Ab, without secondary Ab, and the use of an irrelevant primary Ab.

*Neuropathological analysis in humans.* Three AD patients and three neurologically normal, age-matched controls from the Alzheimer's Disease Research Center of the University of Southern California were evaluated clinically and were followed to autopsy. Included were three males and three females, ranging in age from 69 to 99 years.

Tissue blocks (1 cm³) were obtained postmortem (range 4–7 hours; mean 5 hours.), fixed in 10% neutral buffered formalin (pH 7.3; Sigma Chemical Co.), and

embedded in paraffin or snap-frozen in liquid nitrogen–chilled isopentane. Tissues were sampled from the superior and middle frontal gyrus (Brodmann's area 10), and the cerebellar hemisphere.

Sections were stained with either hematoxylin and eosin or thioflavine S, in a modification of Bielschowsky's silver impregnation method (Gallyas stain). Thioflavine S–stained sections were viewed through a Zeiss fluorescence microscope with a narrow-band, blue/violet filter at 400–455 nm. Examination was performed by two independent observers. Diagnosis of AD was according to a modified protocol from the Consortium to Establish a Registry for Alzheimer's Disease (52).

For immunocytochemical analysis, we used cryostat sections (10 μm) of frontal cortex (Brodmann's area 10) that were air dried. Immunocytochemistry was performed using the avidin-biotin peroxidase complex method (Vector Laboratories Inc., Burlingame, California, USA). Antibodies included $A\beta_{1-40}$, rabbit anti-human, 1:1,000 (1 mg/ml; Chemicon International, Temecula, California, USA); $A\beta_{1-42}$, rabbit anti-human, 1:1,000 (1 mg/ml); the mouse mAb to the heavy chain of human LRP-1 designated 8G1, which is specific for human LRP-1 and recognizes an epitope on the 515-kDa subunit (53), 1:300 (1.5 mg/ml); and CD105 (clone SMG), mouse anti-human, 1:100 (0.1 mg/ml; Serotec Ltd., Oxford, United Kingdom). For single staining with CD105 and LRP, after incubation with primary Ab, sections were washed three times in PBS (pH 7.4), and treated with biotinylated anti-mouse IgG for 30 minutes. After three washes in PBS, slides were incubated with avidin-biotin–horseradish peroxidase complex for 30 minutes and washed three times in PBS. Binding was detected with an SG peroxidase detection kit (blue/gray; Vector Laboratories Inc.). For double labeling, after incubation with $A\beta$ overnight at 4°C, sections were washed three times with PBS and treated with biotinylated anti-rabbit IgG. They were then washed again, and

positivity was detected with NovaRED (Vector Laboratories Inc.). After three washes in PBS, the second primary Ab (LRP or CD-105) was applied, and staining was performed as described for single labeling. Imaging was accomplished using an Axiophot II microscope (Carl Zeiss Inc., Thornwood, New York, USA) equipped with a SPOT digital camera (Diagnostic Instruments Inc., Sterling Heights, Michigan, USA).

## Results

Figure 1a illustrates brain radioactivity-disappearance curves of [14C]inulin and 125I-$A\beta_{1-40}$ (TCA-precipitable 125I radioactivity) studied at a concentration of 60 nM. Clearance of inulin, a reference extracellular fluid (ECF) marker that is neither transported across the BBB nor retained by the brain (40, 43), approximated a single exponential decay, as expected from previous studies. The clearance curve reflecting total efflux of 125I-$A\beta_{1-40}$ from brain was bi-exponential, and was much lower than that for inulin, indicating significant biological transport of $A\beta_{1-40}$ out of the brain. The two components of $A\beta_{1-40}$ efflux, rapid elimination by vascular transport across the BBB into the blood and slow elimination via the ISF flow, were computed from Figure 1a with equations 3 and 4 and are illustrated in Figure 1b. Figure 1b indicates significantly higher clearance of $A\beta$ via BBB transport than via ISF bulk flow.

The half-time ($t_{1/2}$) for brain efflux of $A\beta_{1-40}$ and inulin calculated from Figure 1a and equations 2 and 3 were 25.5 ± 2.0 minutes and 239.0 ± 12.5 minutes, respectively, a 9.4-fold difference (Table 1). The half-time of efflux of $A\beta_{1-40}$ across the BBB was 34.6 ± 3.6 minutes, 6.9-fold faster than by ISF bulk flow. In addition to efflux, there was also a slow, time-dependent retention of $A\beta_{1-40}$ in brain parenchyma with a $t_{1/2}$ of 164.5 minutes. As shown in Table 1, the rate $k$ (min$^{-1}$) of clearance of $A\beta_{1-40}$ from the brain was 7.9-fold higher than that for inulin. The relative contributions of $A\beta_{1-40}$ efflux at 60 nM, by transport across the BBB and by ISF bulk flow based on 5-

## Figure 1

(**a**) Time-disappearance curves of [14C]inulin (open circles) and 125I-$A\beta_{1-40}$ (60 nM; TCA-precipitable 125I radioactivity, filled circles) from the CNS after simultaneous microinjections of tracers into the caudate nucleus in mice. Each point represents the mean ± SD of three to seven animals. (**b**) Two components of 125I-$A\beta_{1-40}$ efflux, vascular transport across the BBB (filled triangles) and transport via ISF bulk flow (open triangles), were computed with equations 3 and 4 using data from **a**. (**c**) Relative contributions to $A\beta_{1-40}$ efflux by its transport across the BBB (open bar), diffusion via ISF bulk flow (filled bar), and retention (gray bar) in the brain were studied at 60 nM concentrations and calculated from the fractional coefficients given in Table 1.
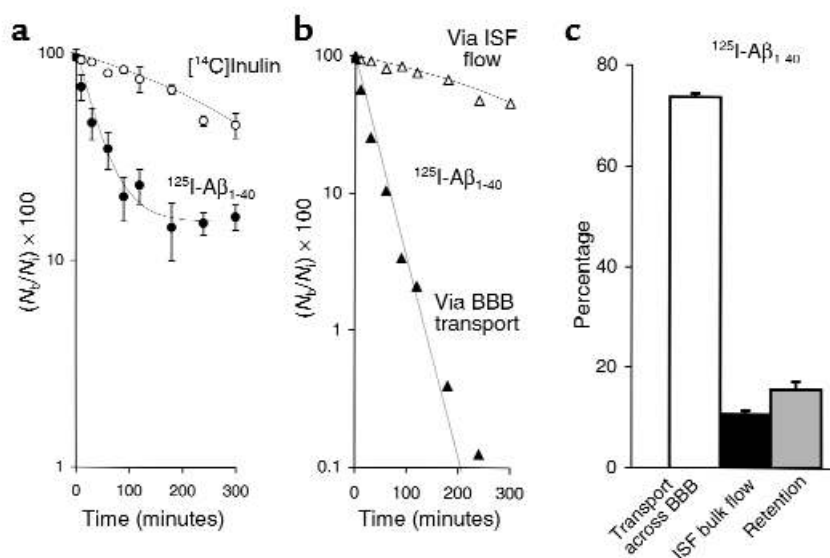
hour measurements, were 73.8% and 10.7% respectively, whereas 15.6% of the dose remained sequestered within the CNS (Figure 1c).

After CNS injection, both tracers reached the CSF; the CSF time-appearance curves are shown in Figure 2a. The amount of $^{125}$I-A$\beta_{1-40}$ (TCA-precipitable $^{125}$I radioactivity) measured in the CSF was lower than that for inulin at each studied timepoint, possibly reflecting active clearance of A$\beta_{1-40}$ from the CSF, as was suggested previously (28). It is noteworthy that at each studied timepoint, the $^{125}$I-labeled material in the CSF was greater than 96% TCA-precipitable, indicating no degradation of the peptide. Both tracers also appeared in plasma (Figure 2b), and higher levels of TCA-precipitable $^{125}$I-A$\beta_{1-40}$ radioactivity than of [$^{14}$C]inulin radioactivity were consistent with active transport of A$\beta_{1-40}$ out of the CNS across the BBB. The absolute amounts of both tracers in the CSF and plasma were low, however, due to relatively rapid clearance from the CSF in comparison to slow ISF bulk flow (29), and significant systemic body clearance (48), respectively.

Figure 3 (a and b) illustrates that $^{125}$I-A$\beta_{1-40}$ was not significantly degraded in brain ISF before its transport across the BBB, as determined by TCA, HPLC, and SDS-PAGE analysis of $^{125}$I radioactivity in brains. The TCA analysis suggests that only 4.2–9.9% of $^{125}$I radioactivity in brains was not TCA-precipitable at different timepoints within 270 minutes of intracerebral microinjection of $^{125}$I-A$\beta_{1-40}$ (Figure 3a). The HPLC analysis of brain radioactivity confirmed the TCA results by indicating that 93.7% of the peptide remains intact in brain ISF at 60 minutes (Figure 3b, right). It is noteworthy that $^{125}$I-A$\beta_{1-40}$ was more than 97% intact at the time of injection, as determined both by the HPLC and TCA analyses. The results were corroborated by SDS-PAGE analysis of lyophilized aliquots of HPLC peaks of brain homogenates at different timepoints after $^{125}$I-A$\beta_{1-40}$ injection, showing a single radioactive band at about 4 kDa (Figure 3b, left). The identity of the radioactive components on gels as A$\beta_{1-40}$ peptide was confirmed by Western blot analysis using anti-A$\beta$ Ab and enhanced chemiluminescence as a detection system (not shown). More than 96% of $^{125}$I radioactivity in the CSF was TCA-precipitable at studied timepoints between 15 minutes and 270 minutes (not shown). In contrast, degradation products of $^{125}$I-A$\beta_{1-40}$ were found in plasma (Figure 3c); the amount of degraded $^{125}$I-A$\beta_{1-40}$ corresponding to non–TCA-precipitable $^{125}$I radioactivity increased from 37.6% to 58.3% during the period from 15 minutes to 120 minutes after intracerebral microinjection of intact $^{125}$I-A$\beta_{1-40}$ (Figure 3c). It is noteworthy that the amount of radioactivity in plasma after 120 minutes was relatively small, and approached the limits of sensitivity of the TCA assay.

**Table 1**
Clearance rates ($k$) for $^{125}$I-A$\beta_{1-40}$ and [$^{14}$C]inulin

| Parameter | $^{125}$I-A$\beta_{1-40}$ | | [$^{14}$C]inulin | |
|---|---|---|---|---|
| | $k$ (min$^{-1}$) | $t_{1/2}$ (min) | $k$ (min$^{-1}$) | $t_{1/2}$ (min) |
| Total efflux | 0.0229 ± 0.0023$^A$ | 25.5 ± 2.0$^A$ | 0.0029 ± 0.0002 | 239.0 ± 12.5 |
| Transport via BBB | 0.0200 ± 0.0023 | 34.6 ± 3.6 | None | None |
| Transport via ISF | 0.0029 ± 0.0002 | 239.0 ± 12.5 | 0.0029 ± 0.0002 | 239.0 ± 12.5 |
| Retention in brain | 0.0042 ± 0.0005 | 164.5 ± 17.6 | None | None |

Data are mean ± SD from 38 individual experiments. Fractional rate ($k$) values were calculated using equations 3 and 4. $^AP < 0.05$ by Student's $t$ test.

Clearance of A$\beta$ in young mice was concentration dependent (Figure 4a). The efflux transport system was half saturated ($K_{1/2}$) at 15.3 nM of A$\beta_{1-40}$. The plateau or maximal clearance capacity was reached between 70 nM and 100 nM, and further increases in A$\beta$ concentration resulted in progressively greater retention of the peptide in the brain. In contrast, clearance of [$^{14}$C]inulin did not change with increasing concentrations of A$\beta$, suggesting a physiologically intact BBB (Figure 4a).

The next set of experiments was designed to characterize the BBB transport system responsible for the transcytosis of A$\beta$. Brains were loaded with $^{125}$I-A$\beta_{1-40}$ at either 12 nM (Figure 4b) or 60 nM (Figure 4c), and clearance was determined at 30 minutes in the absence and presence of several molecular reagents that may act as potential inhibitors of and/or competitors in export. Figure 4b indicates that both the LRP-1 Ab (60 μg/ml) and RAP (200 nM) produced significant (58% and 30%, respectively) reductions in A$\beta$ clearance from the brain compared with vehicle-treated controls; increasing the concentration of RAP to 5 μM decreased A$\beta$ clearance by 44%. A significant (25%) inhibition in A$\beta$ clearance
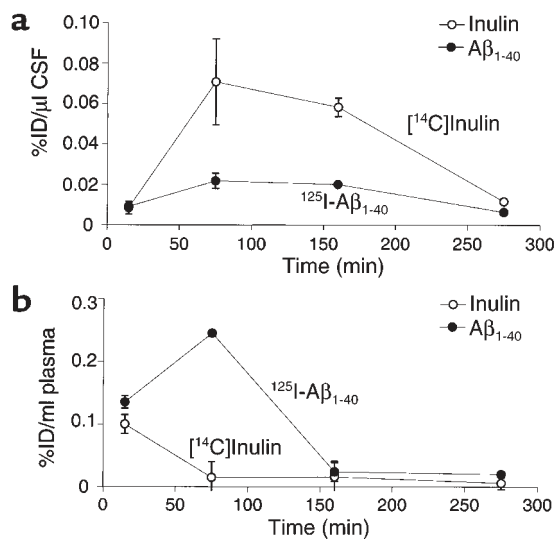


**Figure 2**
Time-appearance curves of [$^{14}$C]inulin (open circles) and $^{125}$I-A$\beta_{1-40}$ (60 nM; TCA-precipitable $^{125}$I radioactivity, filled circles) in the CSF (**a**) and plasma (**b**) after simultaneous microinjections of tracers into the caudate nucleus in mice. Values are expressed as percentages of injected dose (%ID); each point is mean ± SD of three to seven animals.
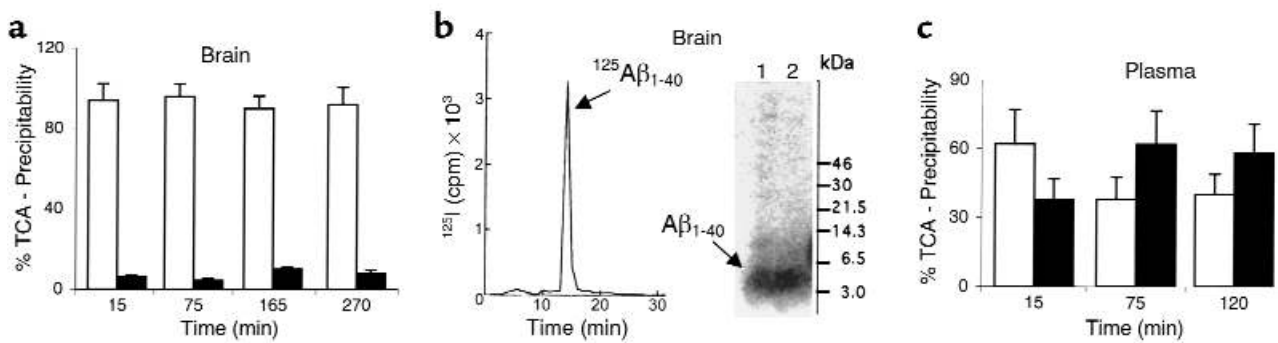
**Figure 3**

(**a**) Brain TCA-precipitable (open bars) and non–TCA-precipitable $^{125}I$ radioactivity (solid bars) after intracerebral microinjections of $^{125}I$-A$\beta_{1-40}$ (60 nM) into the caudate nucleus in mice, expressed as a percentage of total $^{125}I$ radioactivity in the brain; mean ± SD of three to five animals. (**b**) Left panel shows HPLC elution profile of brain tissue 60 minutes after intracerebral microinjection of $^{125}I$-A$\beta_{1-40}$ (60 nM). Separation was performed for 30 mg of brain tissue on a reverse-phase HPLC column, using a 30-minute linear gradient of 25–83% acetonitrile in 0.1% TFA, pH 2. $^{125}I$-A$\beta_{1-40}$ eluted at 52%, corresponding to the elution time of A$\beta_{1-40}$ standard. Right panel shows SDS-PAGE analysis of brain tissue supernatant at 30 minutes (lane 1) and 60 minutes (lane 2) after intracerebral microinjection of $^{125}I$-A$\beta_{1-40}$ (60 nM). The radioactivity in the brain eluted as a single peak on HPLC, with the same retention time as the A$\beta_{1-40}$ standard (data not shown). Aliquots of lyophilized sample were subjected to 10% Tris-tricine SDS-PAGE, transferred to a nitrocellulose membrane, and exposed to x-ray film. (**c**) Plasma TCA-precipitable (open bars) and non–TCA-precipitable $^{125}I$ radioactivity (filled bars) after intracerebral microinjections of $^{125}I$-A$\beta_{1-40}$ (60 nM) into the caudate nucleus in mice, expressed as a percentage of total $^{125}I$ radioactivity in plasma; mean ± SD of three to five animals.

was also obtained in the presence of anti-$\alpha_2$M Ab (20 μg/ml). In contrast, anti–LRP-2 Ab (Figure 4b) and anti-RAGE Ab (Figure 4c) did not affect A$\beta$ clearance. Fucoidin, a specific ligand for SR-A, produced a modest increase in clearance, possibly by blocking the binding of A$\beta$ to parenchymal SR-A receptors, thereby allowing more peptide to be available for clearance. At

higher A$\beta$ loads (Figure 4c), anti–LRP-1 Ab produced a 53% decrease in clearance, similar to that observed at a lower load (Figure 4b), but A$\beta$ recovery approached that of [$^{14}C$]inulin, suggesting drainage of the peptide almost exclusively via ISF bulk flow. Clearance of [$^{14}C$]inulin was not affected by any of the studied molecular reagents. We also demonstrated that BCH, a
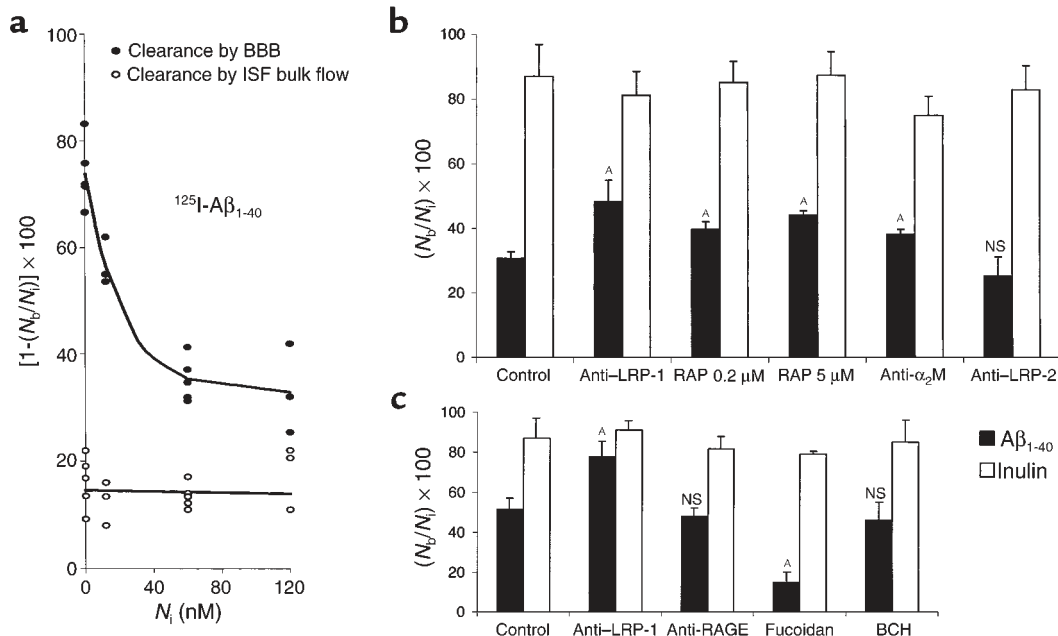


**Figure 4**

(**a**) Concentration-dependent clearance of A$\beta_{1-40}$ from mouse brain. Clearance via BBB transport (filled circles) is shown separately from clearance via ISF bulk flow (open circles). Clearance was determined 30 minutes after simultaneous microinjection of $^{125}I$-A$\beta_{1-40}$ at increasing concentrations (0.05–120 nM) along with [$^{14}C$]inulin into the caudate nucleus. (**b**) Effects of anti–LRP-1 Ab R777 (60 μg/ml), RAP (0.2 and 5 μM), anti-$\alpha_2$M Ab (20 μg/ml), and anti–LRP-2 Ab Rb6286 (60 μg/ml) on brain clearance of $^{125}I$-A$\beta_{1-40}$ at 12 nM, determined 30 minutes after simultaneous microinjection of $^{125}I$-A$\beta_{1-40}$ and [$^{14}C$]inulin. (**c**) Effects of anti–LRP-1 Ab R777 (60 μg/ml), anti-RAGE Ab (60 μg/ml), fucoidin (100 μg/ml), and 2-amino-bicyclo[2.2.1]heptane-2-carboxylic acid (BCH; 10 mM) on brain clearance of $^{125}I$-A$\beta_{1-40}$ at a higher load of 60 nM, determined 30 minutes after simultaneous microinjection of $^{125}I$-A$\beta_{1-40}$ and [$^{14}C$]inulin. Mean ± SD of three to four animals. $^AP < 0.05$; NS, not significant.

substrate that specifically blocks the L system for amino acids, does not affect clearance of Aβ across the BBB. This excludes the possibility that $^{125}$I-Aβ$_{1-40}$ is degraded to $^{125}$I-tyrosine that is then transported out of the CNS instead of $^{125}$I-Aβ$_{1-40}$.

Next, we studied the effect of apoE and aging by determining Aβ clearance in 2-month-old and 9-month-old apoE KO mice and wild-type mice, using two different loads of $^{125}$I-Aβ$_{1-40}$, 12 nM (Figure 5a) and 60 nM (Figure 5b). Figure 5a shows that the clearance of Aβ was reduced by 30% in young apoE KO mice, and by about 55% and 40% in 9-month-old wild-type and apoE KO mice, respectively. These results were confirmed at a higher load of Aβ; the observed decrease in clearance was 46% in 9-month-old apoE KO mice (Figure 5b).

Immunocytochemical studies confirmed abundant expression of LRP-1 in brain microvessels (including capillaries, small venules, and arterioles) in 2-month-old mice (Figure 6a, upper panel; and Figure 6b, upper panel), in addition to significant parenchymal cellular (including neuronal) staining (Figure 6a, upper panel). As shown in the lower panels of Figures 6a and 6b, there was a significant reduction in LRP-1–positive vessels in 9-month-old mice compared with 2-month-old mice; the number of LRP-1–positive vessels dropped from 94% in 2-month-old mice to 52% in 9-month-old mice (Figure 6d, upper panel). Quantitative analysis of LRP-1–positive parenchymal cells (excluding blood vessels) showed a trend toward reduced staining in older animals, though the difference was not statistically significant (Figure 6d, lower panel). Similarly, there was no difference between young and old mice in the number of α$_2$M-positive microvessels or parenchymal cells in the brain (Figure 6c, upper and lower panels, respectively; Figure 6d, lower panel). It is noteworthy that staining for α$_2$M was not able to distinguish between circulating α$_2$M and α$_2$M expressed on microvessels.

Frontal cortex of all AD patients revealed moderate to marked neuritic plaques and Aβ deposits; two of the three showed parenchymal and vascular amyloid. Controls revealed no neuritic plaques or Aβ in the parenchyma, and only meningeal vascular Aβ in one of the three patients. As seen in Figure 7a, staining for LRP-1 in the frontal cortex of control patients revealed moderate vascular staining in capillaries and arterioles, as well as neuronal staining. There was reduced LRP-1 staining in AD tissues, including regions with Aβ$_{1-40}$-positive or Aβ$_{1-42}$-positive plaques and vessels (Figure 7b). However, the immediate subcortical white matter showed more robust vascular staining for LRP-1, and absence of staining for Aβ, in both AD patients and controls (not shown). Anti-CD105, which identifies vascular endothelium, revealed ample staining of capillaries and arterioles of frontal cortex in controls, and moderately reduced numbers of stained vessels in AD tissues. Cerebellum revealed equivalent vascular staining with anti–LRP-1 and anti-CD105 in AD and control sections (not shown). No anti-Aβ$_{1-40}$–positive or Aβ$_{1-42}$–positive staining was seen in either AD or control tissues.
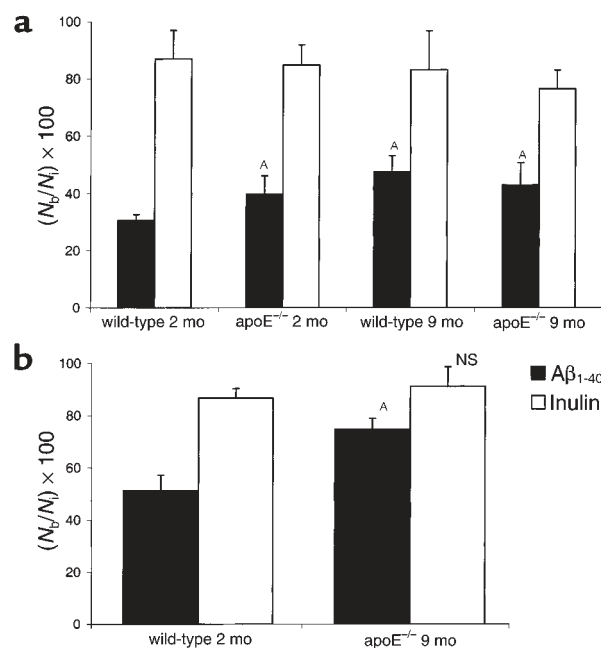


**Figure 5**
(**a**) Effect of apoE genotype and age on brain clearance of $^{125}$I-Aβ$_{1-40}$. Brain clearance of $^{125}$I-Aβ$_{1-40}$ in 2-month-old and 9-month-old wild-type mice and apoE KO mice studied at the lower load of 12 nM $^{125}$I-Aβ$_{1-40}$ (**a**) and a higher load of 60 nM (**b**). In all studies, $^{125}$I-Aβ$_{1-40}$ and [$^{14}$C]inulin were injected simultaneously, and clearance was determined after 30 minutes. Mean ± SD of three to four animals. $^A P < 0.05$; NS, not significant compared with 2-month-old wild-type mice.

## Discussion

This study demonstrates the importance of vascular transport across the BBB in clearing Aβ from the brain into the circulation. Moreover, we provide evidence that this transport mechanism is mediated mainly via LRP-1 in brain microvascular endothelium, and suggest that transport of brain-derived Aβ out of the CNS may be influenced by the LRP-1 ligands α$_2$M and apoE. This vascular clearance mechanism for Aβ is age dependent, and lower clearance rates in older animals correlate with decreased vascular abundance of LRP-1.

The capability of BBB to remove Aβ was significant in younger animals. The elimination time, $t_{1/2}$, for Aβ$_{1-40}$ at 60 nM was 25 minutes, or 9.4-fold faster than for inulin, an ECF marker used to determine the ISF bulk flow rate (40). The major component of the CNS efflux of Aβ was transport across the BBB into the vascular system. The clearance of Aβ across the BBB was dependent on both time and concentration. At very low concentrations, i.e., less than 2 nM as found normally in mouse brain (54–55), Aβ$_{1-40}$ was eliminated from brain at a rate that was on average 3.5-fold faster than when it was present at a load of 60 nM. This may be comparable to concentrations of Aβ$_{1-40}$ found in the brains of transgenic APP animals at 3–4 months of age (54–55). The efflux transport system was half saturated at 15.3 nM of Aβ$_{1-40}$, and appears to be fully saturated at concentrations between 70 nM and 100 nM.

Thus, this efflux transporter may be completely saturated by higher levels of Aβ, as are found in the brains of older transgenic APP animals (54–55), which in turn may lead to vascular accumulation of Aβ and development of prominent deposits of cerebrovascular amyloid, as recently described (56–57).

In this study, we did not observe significant metabolism or degradation of Aβ$_{1-40}$ within 5 hours, in contrast to a recent report suggesting that Aβ$_{1-42}$ is degraded by enkephalinase (neprilysin) in the brain within minutes (28). It may be that Aβ$_{1-40}$ and Aβ$_{1-42}$ are processed differently in the brain. However, the physiological relevance of the proposed degradation mechanism for Aβ$_{1-42}$ (28) remains unclear, because the peptide was studied at extremely high concentrations (~240 μM) that are not found even in brains with severe β-amyloidosis (30). As shown by pharmacological studies, these high concentrations of Aβ may impair local BBB integrity (58–59), which in turn may contaminate brain ISF with blood and/or plasma that possesses Aβ-degrading activity (48), as confirmed in this study.

Consistent with the hypothesis that cytosolic peptidases have little access to Aβ peptides secreted or injected into brain ISF (28) or CSF (29), it has been reported recently that insulin-degrading enzyme (IDE) cannot not degrade Aβ in the brain in vivo after intracerebral injection of radiolabeled peptide (28). This is in contrast to in vitro degradation of $^{125}$I-Aβ$_{1-40}$ by IDE from brain and liver cytosol fractions (60). Because IDE is an intracellular protease, it is not surprising that IDE may not be able to process Aβ from brain ISF, particularly if peptide clearance is faster than its cellular uptake, as suggested by our data and a previous study (28). It is noteworthy that brain endothelial cells in vitro (33) and astrocytes (61) do not catabolize Aβ, in contrast to activated microglial cells that secrete a specific metalloproteinase that degrades Aβ in vitro (61). Neuronal cells in vitro metabolize Aβ via an LRP-1–dependent mechanism that may require apoE or α$_2$M (38). The rate of this degradation, however, is about 50- to 100-fold slower than that occurring via transport across the BBB in vivo.

Transport of Aβ out of the CSF was not associated with significant degradation of peptide in the CSF (29). Lower levels of Aβ$_{1-40}$ than inulin in the CSF may suggest active transport of Aβ from the CSF to the blood, possibly across the choroid plexus or leptomeningeal vessels, as shown previously (29). Higher levels of radiolabeled Aβ in the plasma relative to inulin confirm vascular transport of the peptide out of the CNS. Although our results indicate that brain-derived Aβ could contribute to the pool of circulating peptide, its degradation in plasma, systemic metabolism, and body clearance tend to reduce the levels of circulating peptide, as shown previously (48). Under our experimental con-
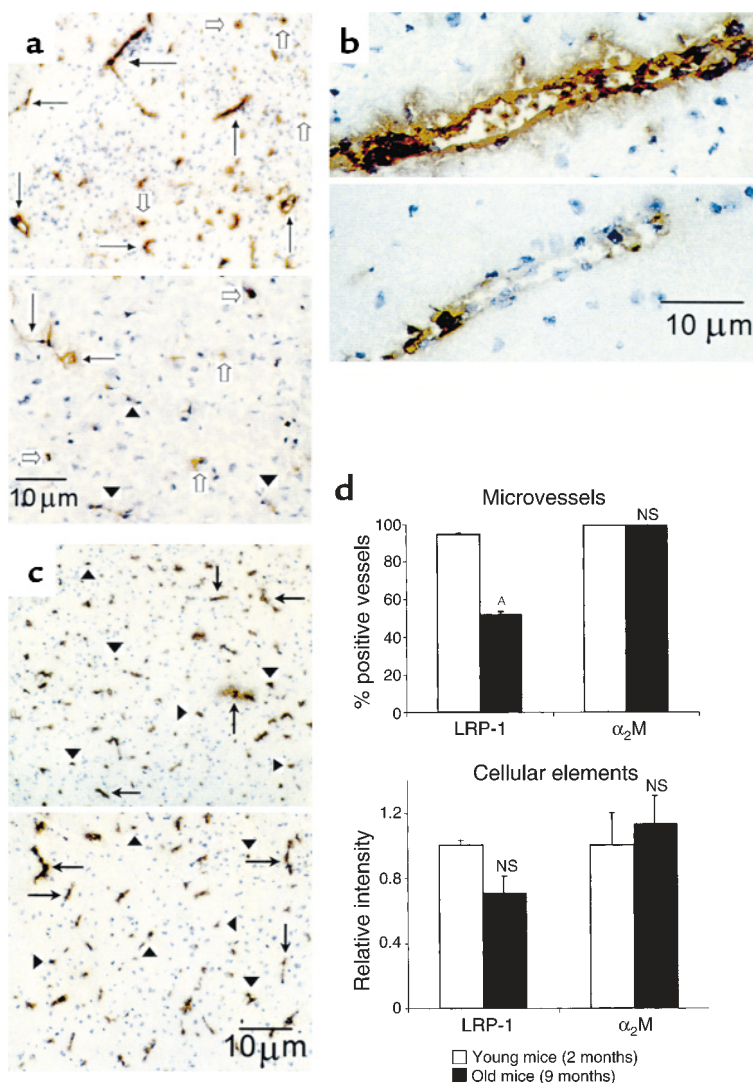


**Figure 6**
(**a**) LRP-1 immunoreactivity in brain microvessels of young (2-month-old; upper panel) and old (9-month-old; lower panel) wild-type mice. Many vessels in young mice stained positive for LRP-1, detected with anti–LRP-1 Ab R777 (5 μg/ml; arrows). There were relatively fewer positive vessels in old mice (arrows), and many weakly positive- or negative-staining vessels (arrowheads). There was no significant difference in the staining of parenchymal cellular elements (open arrows) between the young and old mice. Vessels in young mice stained strongly positive (**b**, upper panel) compared with the faint staining seen in old mice (**b**, lower panel). In contrast, there was no difference in staining for α$_2$M in brain cells (arrowheads) or microvessels (arrows) between young (**c**, upper panel) and old (**c**, lower panel) mice. (**d**) Comparison of LRP-1 and α$_2$M immunoreactivity in brain microvessels (upper panel) and parenchymal cellular elements (lower panel) in young and old wild-type mice. $^{A}P < 0.05$; NS, not significant.

**Figure 7**

LRP-1 expression in human frontal cortex. Brain sections (Brodmann's area 10) of controls (**a** and **c**) reveal well-defined staining of capillaries (arrowheads) and arterioles (arrows) by LRP-1, detected with anti–LRP-1 mAb 8G1 (5 μg/ml) (**a**) and CD105 (**c**). No Aβ staining was present in double-labeled or serially labeled sections (not shown). In contrast, double-labeled sections from AD patients show vessels and plaque cores stained positive with anti-Aβ$_{1-40}$ (brown stain), reduced numbers and intensity of LRP-1 staining of vessels (**b**), and reduced numbers of CD105-labeled vessels (**d**).
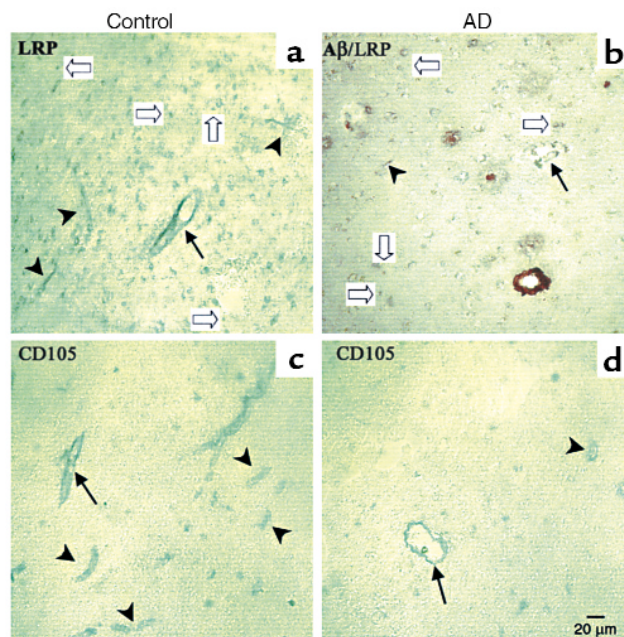


ditions, the levels of radiolabeled Aβ in the circulation were two to three orders of magnitude lower than the brain levels. This makes re-entry of radiolabeled Aβ into the brain very unlikely, because the blood-to-brain transport of Aβ normally operates down the concentration gradient (39, 62–65). In addition, the apoJ system that transports blood-borne Aβ into the brain is saturated under the physiological conditions (64) that may facilitate the efflux of Aβ from the brain. Previous studies have shown that circulating free Aβ is also metabolized during its transport across the BBB (48, 49, 65, 66), possibly by pericytes, which represent a major enzymatic barrier for the transport of several peptides and proteins across the BBB (67).

The affinity of neprilysin for its physiological substrates (e.g., enkephalins, tachykinins, atrial natriuretic peptide) and/or different synthetic peptides is in the low millimolar range (68). In contrast, the levels of Aβ in the brain are normally in the low nanomolar range, and in transgenic mouse models of brain amyloidosis they vary from 40 nM to 250 nM/kg from 3 to 12 months of age (54). Thus, under physiological and/or pathological conditions, Aβ will likely bind to its high-affinity cell-surface receptors (such as RAGE and/or SR-A), and/or high-affinity transport binding proteins (α$_2$M, apoE, and apoJ), which all react with low nanomolar levels of peptide corresponding to their $K_D$ values.

In this study, anti–LRP-1 antibodies inhibited Aβ$_{1-40}$ clearance by about 55%, both at lower (12 nM) and higher loads (60 nM) of the peptide, suggesting the involvement of LRP-1 in vascular elimination of Aβ from the brain. RAP, a chaperone protein that facilitates proper folding and subsequent trafficking of LRP-1 and LRP-2 (69), also inhibited Aβ clearance. RAP binds to multiple sites on LRP and antagonizes binding of all known LRP ligands to both LRP-1 and LRP-2 in vitro (69), as well as to LRP-2 in vivo at the blood side of the BBB (39). In this study, RAP at higher concentrations produced inhibition of Aβ clearance comparable to that produced by an anti–LRP-1 Ab. It is interesting that anti–LRP-1 Ab inhibited vascular transport of Aβ almost completely at higher concentrations of peptide, which may indicate that LRP-1 could be of primary importance in eliminating the peptide from the brain. At a lower load of the peptide (i.e., 12 nM), neither of the molecular reagents was able to abolish clearance of Aβ, which suggests that in addition to LRP-1, there may be an alternative, highly sensitive BBB trans-

port mechanism (or mechanisms) that eliminates the peptide from the brain at very low concentrations. The molecular nature of this putative second transport system is not presently known, although data from this study suggest that RAGE and LRP-2 are unlikely to be involved in rapid elimination of Aβ from brain. The fact that fucoidin, an SR-A ligand, moderately increased clearance of Aβ suggests that inhibition of SR-A receptors in the brain may decrease CNS sequestration of the peptide, thus allowing more peptide to be available for enhanced clearance across the BBB.

A role for LRP-1 in promoting Aβ clearance in vitro in smooth muscle cells, neurons, and fibroblasts via α$_2$M and apoE has been suggested (35–38), although at significantly slower rates than the Aβ transport across the BBB demonstrated in this study. High-affinity in vitro binding of Aβ to α$_2$M and to lipidated apoE3 and apoE4, and a lower-affinity binding to delipidated apoE isoforms has been well documented (23, 70). Binding/uptake studies in mouse embryonic fibroblasts (wild type and deficient in LRP-1), confirmed that free Aβ is not a ligand for LRP-1 (37, 45). The possible role of the two LRP-1 ligands in elimination of Aβ via vascular transport is suggested by inhibition of Aβ clearance with anti-α$_2$M antibodies and by significantly reduced clearance in apoE KO animals (by 30% and 46% at 2 months and 9 months of age, respectively, compared with young wild-type controls). In relation to these findings, it is interesting to note that recent studies have indicated that lack of endogenous mouse apoE in both the APP$^{V717F}$ and APPsw mouse models of AD results in less Aβ deposition and no fibrillar Aβ deposits in the brain (57, 71). This suggests that mouse apoE strongly facilitates Aβ fibrillogenesis. It is possible that mouse apoE also plays a role in clearance of

soluble Aβ across the BBB, as suggested by the current study, but that its ability to influence Aβ aggregation in APP transgenic mice is dominant. In contrast to the effects of mouse apoE, a recent study demonstrates that human apoE isoforms suppress early Aβ deposition in APP[V717F] mice (72). Further studies in this model will be useful to determine whether this suppressive effect of human apoE isoforms on early Aβ deposition is secondary to effects on facilitating Aβ transport across the BBB. Although our study does not rule out the possibility that Aβ clearance by neurons, vascular smooth muscle cells, and fibroblasts shown in vitro (35–38) may also occur in vivo, vascular transport across the BBB seems to be of primary importance for rapid elimination of Aβ from brain in vivo.

Because normal aging is associated with Aβ accumulation in the brain (1), and there is a significant, time-dependent, and progressive accumulation of the peptide with age in transgenic APP animals (54, 55), we postulated that Aβ clearance mechanisms might be impaired in older animals, and are also possibly impaired in elderly humans. Our findings of about 55–65% inhibition of Aβ clearance in 9-month-old wild-type animals compared with young (2-month-old) animals confirmed this hypothesis. Immunocytochemical studies indicated a significant reduction in the number of LRP-1–positive cerebral blood vessels, from 94% in 2-month-old mice to 52% in 9-month-old mice, which correlated well with the observed reductions in the clearance capacities in the two age groups. Interestingly, downregulation of vascular LRP-1 correlated well with regional parenchymal and vascular accumulation of Aβ in brains of Alzheimer's patients compared with age-matched controls. In brain areas where LRP-1 vascular expression remains prominent, such as in the white matter, no accumulation of Aβ was found in Alzheimer's brains.

In conclusion, our data support the concept that the vascular system plays an important role in regulating the levels of Aβ in the brain. Our findings further suggest that if the levels of Aβ in brain extracellular space exceed the transport capacity of the clearance mechanism across the BBB, or if the vascular transport of the peptide were impaired, for example by downregulation of LRP-1, this would result in accumulation of Aβ in the brain, and possibly formation of amyloid plaques. Previous studies from our laboratory and others have demonstrated a major role of the BBB in determining the concentrations of Aβ in the CNS by regulating transport of circulating Aβ (33, 39, 49–51, 62–66). This study extends this hypothesis by showing that vascular transport out of the brain across the BBB may represent a major physiological mechanism that prevents accumulation of Aβ and amyloid deposition in the brain.

### Acknowledgments

1. Wisniewski, T., Ghiso, J., and Frangione, B. 1997. Biology of Aβ amyloid in Alzheimer's disease. *Neurobiol. Dis.* **4**:311–328.
2. Selkoe, D.J. 1997. Alzheimer's disease: genotype, phenotype, and treatments. *Science.* **275**:630–631.
3. Selkoe, D.J. 1998. The cell biology of β-amyloid precursor protein and presenilin in Alzheimer's disease. *Trends Cell Biol.* **8**:447–453.
4. Younkin, S.G. 1998. The role of Aβ42 in Alzheimer's disease. *J. Physiol. (Paris).* **92**:289–292.
5. Roses, A.D. 1998. Alzheimer disease: a model of gene mutations and susceptibility polymorphisms for complex psychiatric diseases. *Am. J. Med. Genet.* **81**:49–57.
6. Hardy, J., Duff, K., Hardy, K.G., Perez-Tur, J., and Hutton, M. 1998. Genetic dissection of Alzheimer's disease and related dementias: amyloid and its relationship to tau. *Nat. Neurosci.* **1**:355–358.
7. Masters, C.L., et al. 1985. Amyloid plaque core protein in Alzheimer disease and Down syndrome. *Proc. Natl. Acad. Sci. USA.* **82**:4245–4249.
8. Prelli, F., Castano, E.M., Glenner, G.G., and Frangione, B. 1988. Differences between vascular and plaque core amyloid in Alzheimer's disease. *J. Neurochem.* **51**:648–651.
9. Roher, A.E., et al. 1993. β-amyloid (1-42) is a major component of cerebrovascular amyloid deposits: implications for the pathology of Alzheimer disease. *Proc. Natl. Acad. Sci. USA.* **90**:10836–10840.
10. Shinkai, Y., et al. 1995. Amyloid β-proteins 1-40 and 1-42(43) in the soluble fraction of extra- and intracranial blood vessels. *Ann. Neurol.* **38**:421–428.
11. Castaño, E.M., et al. 1996. The length of amyloid-β in hereditary cerebral hemorrhage with amyloidosis, Dutch type. Implications for the role of amyloid-β 1-42 in Alzheimer's disease. *J. Biol. Chem.* **271**:32185–32191.
12. Seubert, P., et al. 1992. Isolation and quantification of soluble Alzheimer's amyloid-β peptide from biological fluids. *Nature.* **359**:325–327.
13. Shoji, M., et al. 1996. Production of the Alzheimer amyloid-β protein by normal proteolytic processing. *Science.* **258**:126–129.
14. Vigo-Pelfrey, C., Lee, D., Keim, P., Lieberburg, I., and Schenk, D.B. 1993. Characterization of β-amyloid peptide from human cerebrospinal fluid. *J. Neurochem.* **61**:965–968.
15. Tabaton, M., et al. 1994. Soluble amyloid β-protein is a marker of Alzheimer amyloid in brain but not in cerebrospinal fluid. *Biochem. Biophys. Res. Commun.* **200**:1598–1603.
16. Kuo, Y.M., et al. 1996. Water-soluble Aβ (N-40, N-42) oligomers in normal and Alzheimer disease brains. *J. Biol. Chem.* **271**:4077–4081.
17. Ghiso, J., et al. 1993. The cerebrospinal-fluid soluble form of Alzheimer's amyloid-β is complexed to SP-40, 40 (apolipoprotein J), and inhibitor of the complement membrane-attack complex. *Biochem. J.* **293**:27–30.
18. Matsubara, E., Frangione, B., and Ghiso, J. 1995. Characterization of apolipoprotein J-Alzheimer's Aβ interaction. *J. Biol. Chem.* **270**:7563–7567.
19. Yang, D.S., Smith, J.D., Zhou, Z., Gandy, S.E., and Martins, R.N. 1997. Characterization of the binding of amyloid-β peptide to cell culture-derived native apolipoprotein E2, E3, and E4 isoforms and to isoforms from human plasma. *J. Neurochem.* **68**:721–725.
20. Schwarzman, A.L., et al. 1994. Transthyretin sequesters amyloid β-protein and prevents amyloid formation. *Proc. Natl. Acad. Sci. USA.* **91**:8368–8372.
21. Matsubara, E., et al. 1999. Lipoprotein-free amyloidogenic peptides in plasma are elevated in patients with sporadic Alzheimer's disease and Down's syndrome. *Ann. Neurol.* **45**:537–541.
22. Biere, A.L., et al. 1996. Amyloid β-peptide is transported on lipoproteins and albumin in human plasma. *J. Biol. Chem.* **271**:32916–32922.
23. Du, Y., et al. 1997. β2-Macroglobulin as a β-amyloid peptide-binding plasma protein. *J. Neurochem.* **69**:299–305.
24. Busciglio, J., Gabuzda, D.H., Matsudaira, P., and Yanker, B.A. 1993. Generation of β-amyloid in the secretory pathway in neuronal and non-neuronal cells. *Proc. Natl. Acad. Sci. USA.* **90**:2092–2096.
25. Naslund, J., et al. 1994. Relative abundance of Alzheimer Aβ amyloid peptide variants in Alzheimer disease and normal aging. *Proc. Natl. Acad. Sci. USA.* **91**:8378–8382.
26. Teller, J.K., et al. 1996. Presence of soluble amyloid β-peptide precedes amyloid plaque formation in Down's syndrome. *Nat. Med.* **2**:93–95.
27. Suzuki, N., et al. 1994. High tissue content of soluble amyloid-β 1-40 is linked to cerebral amyloid angiopathy. *Am. J. Pathol.* **145**:452–460.
28. Iwata, N., et al. 2000. Identification of the major Aβ1-42-degrading catabolic pathway in brain parenchyma: suppression leads to biochemical and pathological deposition. *Nat. Med.* **6**:143–150.

29. Ghersi-Egea, J.F., et al. 1996. Fate of cerebrospinal fluid-borne amyloid β-peptide: rapid clearance into blood and appreciable accumulation by cerebral arteries. *J. Neurochem.* **67**:880–883.

30. Zlokovic, B.V., Yamada, S., Holtzman, D., Ghiso, J., and Frangione, B. 2000. Clearance of amyloid β-peptide from brain: transport or metabolism? *Nat. Med.* **6**:718–719.

31. Rosenberg, R.N. 2000. The molecular and genetic basis of AD: the end of the beginning. *Neurology.* **54**:2045–2054.

32. Yan, S.D., et al. 1996. RAGE and amyloid-β peptide neurotoxicity in Alzheimer's disease. *Nature.* **382**:685–691.

33. Mackic, J.B., et al. 1998. Human blood-brain barrier receptors for Alzheimer's amyloid-β$_{1-40}$: asymmetrical binding, endocytosis and transcytosis at the apical side of brain microvascular endothelial cell monolayer. *J. Clin. Invest.* **102**:734–743.

34. Paresce, D.M., Ghosh, R.N., and Maxfield, F.R. 1996. Microglial cells internalize aggregates of the Alzheimer's disease amyloid β-protein via a scavenger receptor. *Neuron.* **17**:553–565.

35. Urmoneit, B., et al. 1997. Cerebrovascular smooth muscle cells internalize Alzheimer amyloid β-protein via a lipoprotein pathway: implications for cerebral amyloid angiopathy. *Lab. Invest.* **77**:157–166.

36. Jordan, J., et al. 1998. Isoform-specific effect of apolipoprotein E on cell survival and β-amyloid-induced toxicity in rat hippocampal pyramidal neuronal cultures. *J. Neurosci.* **18**:195–204.

37. Narita, M., Holtzman, D.M., Schwartz, A.L., and Bu, G. 1997. α$_2$-macroglobulin complexes with and mediates the endocytosis of β-amyloid peptide via cell surface low-density lipoprotein receptor-related protein. *J. Neurochem.* **69**:1904–1911.

38. Qiu, Z., Strickland, D.K., Hyman, B.T., and Rebeck, G.W. 1999. α$_2$-macroglobulin enhances the clearance of endogenous soluble β-amyloid peptide via low-density lipoprotein receptor-related protein in cortical neurons. *J. Neurochem.* **73**:1393–1398.

39. Zlokovic, B.V., et al. 1996. Glycoprotein 330/megalin: probable role in receptor-mediated transport of apolipoprotein J alone and in a complex with Alzheimer's disease amyloid β at the blood-brain and blood-cerebrospinal fluid barriers. *Proc. Natl. Acad. Sci. USA.* **93**:4229–4236.

40. Yamada, S., dePasquale, M., Patlak, C.S., and Cserr, H.F. 1991. Albumin outflow into deep cervical lymph from different regions of rabbit brain. *Am. J. Physiol.* **261**:H1197–H1204.

41. Strittmater, W., and Roses, A. 1996. Apolipoprotein E and Alzheimer's disease. *Annu. Rev. Neurosci.* **19**:53–77.

42. Blacker, D., et al. 1998. α2-macroglobulin is genetically associated with Alzheimer's disease. *Nat. Gen.* **19**:357–360.

43. Zlokovic, B.V., Davson, H., Preston, J.E., and Segal, M.B. 1987. Effects of aluminum on cerebrospinal fluid secretion. *Exp. Neurol.* **98**:436–452.

44. Kounnas, M.Z., et al. 1992. The α$_2$-macroglobulin receptor/low density lipoprotein receptor-related protein binds and internalizes *Pseudomonas* exotoxin A. *J. Biol. Chem.* **267**:12420–12423.

45. Kounnas, M.Z., et al. 1995. LDL receptor-related protein, a multifunctional ApoE receptor, binds secreted β-amyloid precursor protein an mediates its degradation. *Cell.* **82**:331–340.

46. Mikhailenko, I., Kounnas, M.Z., and Strickland, D.K. 1995. Low density lipoprotein receptor-related protein/α 2-macroglobulin receptor mediates the cellular internalization and degradation of thrombospondin. A process facilitated by cell-surface proteoglycans. *J. Biol. Chem.* **270**:9543–9549.

47. Kounnas, M.Z., Haudenschild, C.C., Strickland, D.K., and Argraves, W.S. 1994. Immunological localization of glycoprotein 330, low density lipoprotein receptor related protein and 39 kDa receptor associated protein in embryonic mouse tissues. *In Vivo.* **8**:343–351.

48. Mackic, J.B., et al. 1998. Cerebrovascular accumulation and increased blood-brain barrier permeability to circulating Alzheimer's amyloid β-peptide in aged squirrel monkey with cerebral amyloid angiopathy. *J. Neurochem.* **70**:210–215.

49. Maness, L.M., Banks, W.A., Podlisny, M.B., Selkoe, D.J., and Kastin, A.J. 1994. Passage of human amyloid-β protein 1-40 across the murine blood-brain barrier. *Life Sci.* **55**:1643–1650.

50. Poduslo, J.F., Curran, G.L., Haggard, J.J., Biere, A.L., and Selkoe, D.J. 1997. Permeability and residual plasma volume of human, Dutch variant, and rat amyloid β-protein 1-40 at the blood-brain barrier. *Neurobiol. Dis.* **4**:27–34.

51. Martel, C.L., et al. 1997. Isoform-specific effects of apolipoproteins E2, E3, E4 on cerebral capillary sequestration and blood brain barrier transport of circulating Alzheimer's amyloid β. *J. Neurochem.* **69**:1995–2004.

52. Hyman, B.T., and Trojanowski, J.Q. 1997. Consensus recommendations for the postmortem diagnosis of Alzheimer disease from the National Institute on Aging and the Reagan Institute Working Group on diagnostic criteria for the neuropathological assessment of Alzheimer disease. *J. Neuropathol. Exp. Neurol.* **56**:1095–1097.

53. Strickland, D.K., et al. 1990. Sequence identity between the α$_2$-macroglobulin receptor and low density lipoprotein receptor-related protein suggests that this molecule is a multifunctional receptor. *J. Biol. Chem.* **265**:17401–17404.

54. Hsiao, K., et al. 1996. Correlative memory deficits, Aβ elevation, and amyloid plaques in transgenic mice. *Science.* **274**:99–102.

55. Holcomb, L., et al. 1998. Accelerated Alzheimer-type phenotype in transgenic mice carrying both mutant amyloid precursor protein and presenilin 1 transgenes. *Nat. Med.* **4**:97–100.

56. Calhoun, M.E., et al. 1999. Neuronal overexpression of mutant amyloid precursor protein results in prominent deposition of cerebrovascular amyloid. *Proc. Natl. Acad. Sci. USA.* **96**:14088–14093.

57. Holtzman, D.M., et al. 2000. ApoE facilitates neuritic and cerebrovascular plaque formation in the APPsw mouse model of Alzheimer's disease. *Ann. Neurol.* **47**:739–747.

58. Blanc, E.M., Toborek, M., Mark, R.J., Hennig, B., and Mattson, M.P. 1997. Amyloid β-peptide induces cell monolayer albumin permeability, impairs glucose transport, and induces apoptosis in vascular endothelial cells. *J. Neurochem.* **68**:1870–1881.

59. Thomas, T., Thomas, G., McLendon, C., Sutton, T., and Mullan, M. 1996. β-amyloid mediated vasoactivity and vascular endothelial damage. *Nature.* **380**:168–171.

60. Kurochkin, I.V., and Goto, S. 1994. Alzheimer's β-amyloid peptide specifically interacts with and is degraded by insulin degrading enzyme. *FEBS Lett.* **345**:33–37.

61. Mentlein, R., Ludwig, R., and Martensen, I. 1998. Proteolytic degradation of Alzheimer's disease amyloid β-peptide by a metalloproteinase from microglia cells. *J. Neurochem.* **70**:721–726.

62. Zlokovic, B.V., et al. 1993. Blood-brain barrier transport of circulating Alzheimer's amyloid-β. *Biochem. Biophys. Res. Commun.* **197**:1034–1040.

63. Ghilardi, J.R., et al. 1996. Intra-arterial infusion of [$^{125}$I]Aβ$_{1-40}$ labels amyloid deposits in the aged primate brain in vivo. *Neuroreport.* **7**:2607–2611.

64. Shayo, M., McLay, R.N., Kastin, A.J., and Banks, W.A. 1997. The putative blood-brain barrier transporter for the β-amyloid binding protein apolipoprotein J is saturated at physiological concentrations. *Life Sci.* **60**:L115–L118.

65. Martel, C.L., Mackic, J.B., McComb, J.G., Ghiso, J., and Zlokovic, B.V. 1996. Blood-brain barrier uptake of the 40 and 42 amino acid sequences of circulating Alzheimer's amyloid-β in guinea pigs. *Neurosci. Lett.* **206**:157–160.

66. Saito, Y., Buciak, J., Yang, J., and Pardridge, W.M. 1995. Vector-mediated delivery of $^{125}$I-labeled β-amyloid peptide Aβ 1-40 through the blood-brain barrier and binding to Alzheimer's disease amyloid to the Aβ$_{1-40}$/ vector complex. *Proc. Natl. Acad. Sci. USA.* **92**:10227–10231.

67. Krause, D., Kunz, J., and Dermietzel, R. 1993. Cerebral pericytes: a second line of defense in controlling blood-brain barrier peptide metabolism. *Adv. Exp. Med. Biol.* **331**:149–152.

68. Hersh, L.B., and Morihara, K. 1986. Comparison of subsite specificity of the mammalian neutral endopeptidase 24.11 (enkephalinase) to the bacterial neutral endopeptidase thermolysin. *J. Biol. Chem.* **261**:6433–6437.

69. Bu, G., and Rennke, S. 1996. Receptor-associated protein is a folding chaperone for low-density lipoprotein receptor-related protein. *J. Biol. Chem.* **271**:22218–22224.

70. Tokuda, T., et al. 2000. Lipidation of apolipoprotein E influences its isoform-specific interaction with Alzheimer's amyloid β-peptides. *Biochem. J.* **348**:359–365.

71. Bales, K.R., et al. 1999. Apolipoprotein E is essential for amyloid deposition in the APP(V717F) transgenic mouse model of Alzheimer's disease. *Proc. Natl. Acad. Sci. USA.* **96**:15233–15238.

72. Holtzman, D.M., et al. 1999. In vivo expression of apolipoprotein E reduces amyloid β deposition in a mouse model of Alzheimer's disease. *J. Clin. Invest.* **103**:R15–R21.